Solvent-Assisted Processing of MOCA-Extended Polyurethanes: Toward Enhanced Processability and Tunable Properties

Dongwei Chu, Heng Li, Mingming Zhou, Huiyu Zhao, Jingjiang Sun* and Qingfu Wang*

Key Laboratory of Rubber-plastics Ministry of Education, School of Polymer Science and Engineering, Qingdao University of Science and Technology, Zhengzhou Rd. 53, Qingdao CN-266042, China

Abstract: To regulate the rapid reaction kinetics of 3,3'-dichloro-4,4'-diaminodiphenylmethane (MOCA) chain extension in cast polyurethane (CPU) elastomers, a solvent casting strategy was developed. By dissolving MOCA in ethyl acetate, the pot life was significantly extended from <20 s to >10 min, enabling homogeneous mixing and processing. A series of CPUs were synthesized using polytetrahydrofuran ether glycol (PTMEG-1000) as the soft segment and different diisocyanates (TDI and MDI-50) as the hard segment monomers. The hard segment content exerted a significant influence on the mechanical properties, with an n_{TDI}: n_{PTMEG} ratio of 2: 1 yielding an optimal tensile strength of 50.74 MPa. Furthermore, the hard segment composition played a critical role: MDI-50-based CPUs exhibited superior thermal stability. Blending TDI with MDI-50 allowed for tunable properties, and a molar ratio of n_{MDI}: n_{TDI} = 5: 5 resulted in the poorest mechanical properties (35.96 MPa). This work provides a practical and effective approach to tailoring the comprehensive properties of high-performance CPU elastomers for demanding applications.

Keywords: Cast polyurethane elastomers, Solvent casting, MOCA, Hard segments, Mechanical properties.

1. INTRODUCTION

From daily-used sofa cushions to industrial pipeline insulation layers, and from automotive shock-absorbing components to surgically used biocompatible catheters, polyurethane (PU) has become a key polymeric material bridging consumer life and industrial manufacturing due to its unique urethane molecular architecture [1]. Since Otto Bayer and coworkers first synthesized PU using 1,6-hexamethylene diisocyanate and 1,4-butanediol as raw materials in 1937 [2], this material has undergone nearly a century of technological evolution. Through adjusting the molecular ratio between hard and soft segments and optimizing the chain extender type, PU has achieved a performance leap from ultra-soft foams to high-strength elastomers. It represents one of the few synthetic material systems capable of integrating the rigidity of plastics with the elasticity of rubber [3-5], with its diversified forms encompassing foam plastics, elastomers, coatings, adhesives, and other specialized categories [6-10]. Cast polyurethane elastomer (CPU), processed via casting molding, is particularly suited for fabricating elastomers with complex geometries and those challenging to process by other means [11]. Elastomers produced by this method exhibit outstanding mechanical properties and wear resistance, making them widely applicable in areas such as industrial rollers and other aspects [12].

3,3'-Dichloro-4,4'-diaminodiphenylmethane (MOCA) is a typical aromatic diamine chain extender. It appears as white to pale yellow needle-like crystal at room temperature, with a melting point of approximately 101-104 ℃, and requires heating to around 120 ℃ for melt processing. MOCA can form a well-compatible reaction system with prepolymers and react with terminal isocyanate groups to generate hard segments composed of urea linkages with high cohesion energy, thereby enabling precise regulation of the crosslinked structure of PU [13]. The key advantages of MOCA as a chain extender lie in its significant enhancement of PU performance: it enables elastomers to achieve tensile strength exceeding 35 MPa, improves wear resistance by 8- to 10-fold compared to conventional rubber [14], and allows Shore A hardness to be continuously adjusted from 80 to 95 by varying its content, where the optimal performance is observed at an extension coefficient between 0.85 and 0.95 [15-17]. These materials also exhibit low permanent deformation and remain cost-effective, making them suitable for demanding applications such as industrial rubber rollers and mining screen plates. However, MOCA also presents notable drawbacks as a chain extender [18]. During the chain extension reaction with prepolymers, the reactivity of its amino groups is strongly influenced by temperature [19]. Excessively high temperatures accelerate the chain extension rate [20-22], resulting in a sharp increase in material viscosity, reduced flowability, and defects such as incomplete mold filling or material shortage in the final products [23, 24]. Conversely, overly low temperatures reduce production efficiency and negatively affect the mechanical properties and service life of the products [25].

In this study, to overcome the issues of excessively fast reaction kinetics and nonuniform mixing

*Address Correspondence to this Author at the Key Laboratory of Rubber-plastics Ministry of Education, School of Polymer Science and Engineering, Qingdao University of Science and Technology, Zhengzhou Rd. 53, Qingdao CN-266042, China;
E-mail: wangqf@qust.edu.cn; sunjij@qust.edu.cn

Received on 02-12-2025 Accepted on 05-01-2026 Published on 10-01-2026

E-ISSN: 000-000/26

encountered when using MOCA as a chain extender in casting processes, a solvent casting method was adopted [26, 27]. Specifically, solvents such as N,N-dimethylacetamide (DMAC) or ethyl acetate were used to dissolve solid MOCA at low temperature. The resulting solution was then homogeneously blended with prepolymer, after which the solvent was removed under vacuum drying, followed by high-temperature curing to afford the final CPU product. This approach enables the chain extension to proceed at a reduced temperature, which not only lowers energy consumption and volatile emissions but also mitigates an excessively rapid reaction rate. With this strategy, the pot life of casting system after MOCA addition was extended from approximately 20 s to more than 10 min. Moreover, the low viscosity of the reaction mixture facilitates uniform casting in polytetrafluoroethylene molds. Using this method, CPU products were successfully synthesized based on toluene diisocyanate (TDI), diphenylmethane diisocyanate (MDI-50), and polytetrahydrofuran ether glycol-1000 (PTMEG-1000) as prepolymers, with MOCA as the chain extender. By adjusting the ratio of MDI-50 to TDI, the influence of hard segment composition on the mechanical properties, wear resistance, and thermal stability of CPUs was systematically investigated (Scheme **1**).

2. EXPERIMENTAL SECTION

2.1. Materials

Diphenylmethane diisocyanate (MDI-50) (99%, Wanhua Chemical Group Co., Ltd.), ethyl acetate (AR, ≥99.5%, Energy Chemical), N,N-dimethylacetamide (DMAC) (≥99.5%, Energy Chemical), polytetrahydrofuran ether glycol (PTMEG-1000) (M_n = 1000 g/mol, MREDA), toluene-2,4-diisocyanate (TDI) (99%, ADAMAS), 3,3'-dichloro-4,4'-diaminodiphenylmethane (MOCA) (98%, MACKLIN).

2.2. General Procedure for CPU Preparation

(1) Preparation of CPUs with Different Hard Segment Contents

PTMEG-1000 was added into a three-neck flask and dried under vacuum at 110 °C for 2 h. After cooling to 60°C, a quantitative amount of TDI was added. The reactor was purged with nitrogen for 15 min, then gradually heated to 80 °C and stirred for 1.5 h under a nitrogen atmosphere to afford the prepolymer. A predetermined quantity of MOCA was dissolved in DMAC or ethyl acetate, and subsequently added into the prepolymer, followed by thorough stirring to achieve a homogeneous mixture. The mixture was cast into a polytetrafluoroethylene mold; which was then transferred to a vacuum oven and subjected to vacuum defoaming at 60 °C for 5 min. After defoaming, the mold was cured in an oven at 100 °C for 12 h. The cured samples were aged for 5 days prior to performance testing.

The formulation used for preparation is summarized in Table **1** (chain extension coefficient = 0.95).

$$HS\% = \frac{n_1 M_1 + n_3 M_3}{n_1 M_1 + n_2 M_2 + n_3 M_3}$$

HS% represents the content of the hard segment in polyurethane, n_1 is the amount of isocyanate, M_1 is the relative molecular mass of isocyanate, n_2 is the amount of polyol, M_2 is the relative molecular mass of polyol, n_3 is the amount of chain extender, and M_3 is the relative molecular mass of the chain extender.

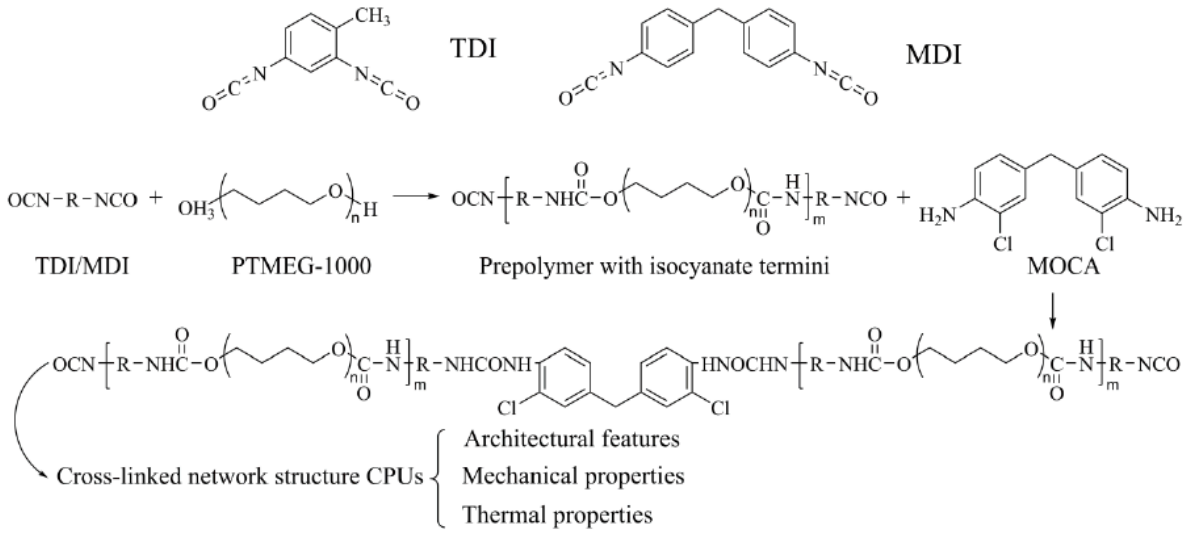

Scheme 1: Schematic illustration of preparation of CPUs.

Table 1: Formulations of CPU with Different Hard Segment Contents

Sample code	n_{PTMEG}: n_{TDI}: n_{MOCA}	Hard segment content
PU1	1: 1.6: 0.57	30.49%
PU2	1: 1.8: 0.76	33.93%
PU3	1: 2.0: 0.95	37.56%
PU4	1: 2.2: 1.14	40.73%
PU5	1: 2.4: 1.33	43.59%

(2) Preparation of CPUs with Different Hard Segment Compositions

Using a fixed molar ratio of isocyanate to PTMEG-1000 at 2:1, CPUs were prepared according to the procedure described in section (1) by varying the molar ratio of MDI-50 to TDI. The corresponding formulation is shown in Table **2**.

2.3. Measurements

Fourier transform infrared (FTIR) spectroscopy was performed on a Bruker VERTEX-70 spectrometer (Germany). Thermogravimetric analysis (TGA) was conducted using a Mettler Toledo TGA2 thermogravimetric analyzer (USA) at a heating rate of 10 °C/min under a nitrogen atmosphere. Hardness was measured in accordance with GB/T 531-2008. Tensile strength and tear strength were carried out on an AI-7000-SU1 universal testing machine (Gaotie Testing Instruments Co., Ltd.) following B/T 528-2009 and GB/T 529-2008, respectively, with a crosshead speed of 500 mm/min (Measure five samples and take the average; Tear strength error < 3%, tensile strength error < 5%). Differential scanning calorimetry (DSC) was performed on a NETZSCH DSC204F1 instrument (Germany) in accordance with GB/T 29611-2013, scanning from -80 °C to 100 °C at 10 °C/min. Rebound resilience at room temperature was evaluated using a GT-7042-RDH rubber rebound tester (Gaotie Technology Co., Ltd.) with reference to GB/T 1681-2009 (Measure two samples and take the average; error < 5%). DIN abrasion resistance was determined following GB/T 9867-2008 (Measure three samples and take the average; error < 5%). The actual mass of samples before and after abrasion testing was measured using a Precisa-XB220A electronic analytical balance.

3. RESULTS AND DISCUSSION

3.1. Solvent Casting Strategy for Regulating the Chain Extension Rate

The conventional prepolymer method involves direct addition of molten MOCA (the melting temperature of MOCA is approximately 120℃) into the prepolymer, which, due to the elevated temperature and high system viscosity, results in an excessively rapid chain extension reaction, a sharp rise in viscosity, and gelation within a short period (<20 s) (Figure **1D**). Herein, a solvent casting method was applied. MOCA was dissolved in a solvent, enabling the chain extension reaction to proceed at or near room temperature. Moreover, the solvent addition lowered the viscosity of the reaction system, thereby preventing gelation for 10 min (Figure **1A**). While highly polar solvents such as DMAC are commonly employed in such solvent-based approaches owning to their strong solubility, requiring only about 1 mL of DMAC for dissolving 1.5 g of MOCA. However, the strong hygroscopicity of DMAC can lead to side reactions with isocyanate groups, adversely affecting the mechanical properties of the CPU [28]. There were issues of poor repeatability in the experiments. For instance, when the air humidity increased, the average tensile strength of the synthesized polyurethane decreased from 42 MPa to 35 MPa, and the errors among multiple samples were significant (>15%). Therefore, ethyl acetate was selected as an alternative. Although its lower polarity

Table 2: Formulations of CPU with Different Hard Segment Compositions

Sample Code	n_{PTMEG}: n_{MDI}: n_{TDI}: n_{MOCA}	Hard Segment Content
PU6	1: 2 :0 :0.95	43.25%
PU7	1: 1.4: 0.6: 0.95	41.75%
PU8	1: 1: 1: 0.95	40.70%
PU9	1: 0.6: 1.4: 0.95	39.61%

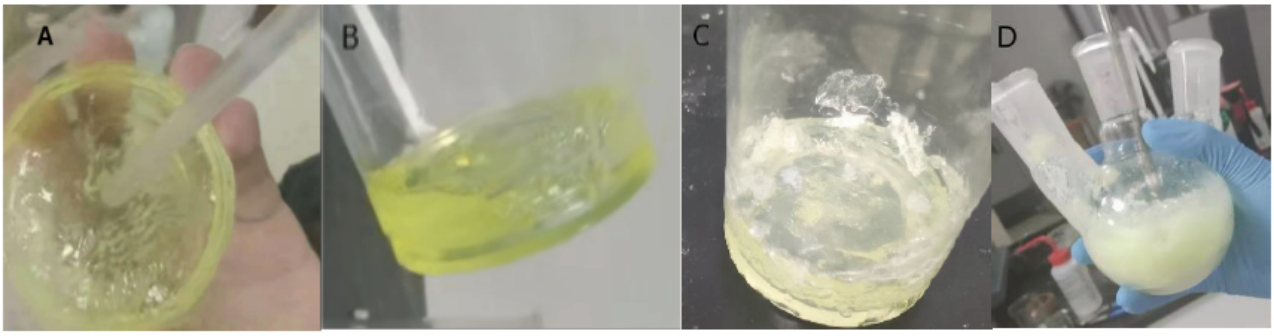

Figure 1: Gelation behavior of CPU systems prepared with different amounts of ethyl acetate: (**A**) sample a (lower solvent content) at 10 min, (**B**) sample b (higher solvent content) at 30 min, and (**C**) sample b at 1 h.(**D**)The reaction phenomenon of the prepolymer method (Reaction time<20s).

necessitates a slightly larger volume (ca. 2 mL ethyl acetate per gram of MOCA), it offers a lower boiling point, easier removal, and low moisture absorption, contributing to easier processing and more stable CPU performance. To illustrate the effect of solvent amount, two equal portions of prepolymers (denoted a and b) were prepared: sample a, mixed with MOCA dissolved in a minimal amount of ethyl acetate, gelled within 10 min (Figure **1A**), while sample b, prepared with twice the solvent volume, only exhibited a slight viscosity increase in the same period. After 30 min, sample b formed a non-flowing gel (Figure **1B**), and after 1 h, both samples had solidified to a similar solid state (Figure **1C**).

3.2. Influence of Hard Segment Content on CPU Properties

CPU elastomers with different hard segment contents were prepared by adjusting the TDI content, and their chemical structures were studied by Fourier transform infrared (FTIR) spectroscopy (Figure **2**). The spectra reveal the absence of an absorption peak around 2269 cm^{-1}, confirming complete consumption of the -NCO groups. Characteristic absorption bands associated with the urethane linkage are observed at approximately 3300 cm^{-1} (N-H stretching) and 1535 cm^{-1} (N-H bending), respectively. The symmetric and asymmetric stretching vibrations of $-CH_2$ appear at 2944 cm^{-1} and 2864 cm^{-1}, respectively. the carbonyl stretching vibration around 1700 cm^{-1} splits into two peaks, which can be attributed to hydrogen-bonding interections [29, 30]. Additionally, the stretching vibration absorption peak of C-O-C is detected near 1111 cm^{-1}. These characteristic features collectively confirm the successful synthesis of the CPU elastomers with different hard segment contents.

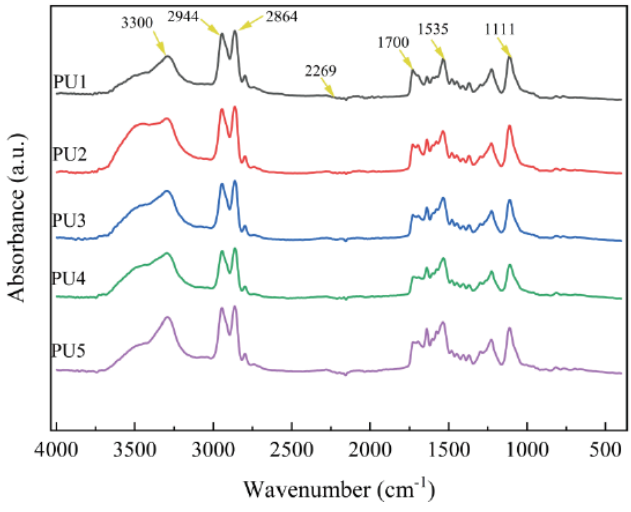

Figure 2: FTIR spectra of PU1 – PU5.

Figure **3** presents the thermogravimetric analysis (TGA) and derivative thermogravimetric (DTG) curves of TDI-based CPU elastomers with different hard segment contents. The thermal degradation process of all samples proceeds mainly through four distinct stages. The first stage, from the initial temperature to approximately 240 °C, is attributed to the volatilization or decomposition of low-molecular-weight substances trapped within the polymer matrix. The second stage (240~370 °C) involves the decomposition of soft segment chains, accompanied by the dissociation of urethane bonds (-NHCOO-) into volatile fragments. At 95% mass retention, the sample of PU1 exhibits a relatively higher decomposition temperature, and a similar trend is observed at 50% mass retention. In the third stage (370~435 °C), degradation occurs primarily in the hard segment domains, along with decomposition of other residual polymers structures. The final stage (435~600 °C) corresponds to further breakdown and carbonization of the remaining char, with only minimal mass loss. Overall, the TGA results indicate a slight decrease in thermal stability with increasing hard segment content, though the differences among the samples remain relatively small.

The differential scanning calorimetry (DSC) curves of CPU elastomers with different hard segment

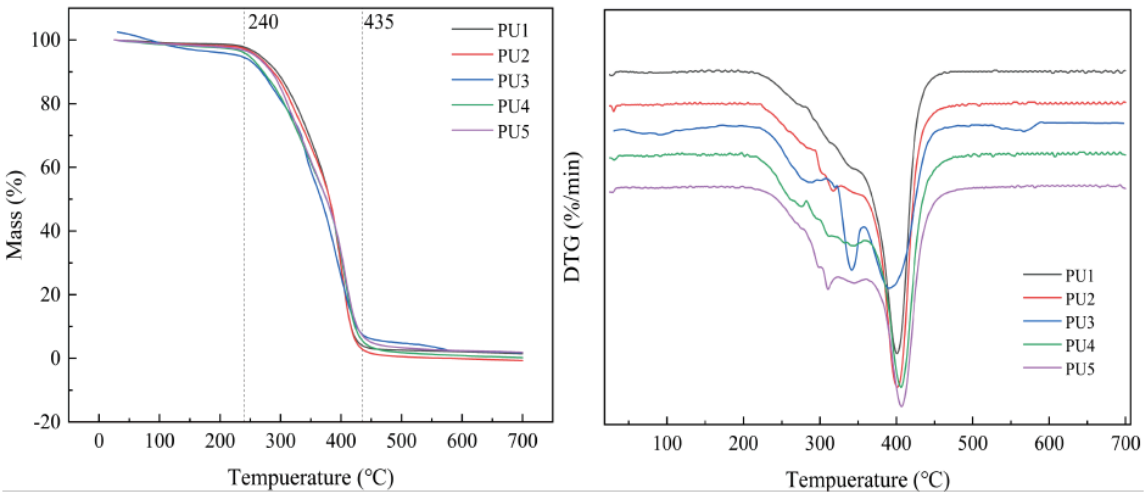

Figure 3: TGA curves (Left) and DTG curves (right) of PU1 – PU5.

contents are shown in Figure **4**, from which the glass transition temperature (T_g) of each sample was determined. The T_g of the CPU is predominantly governed by the composition and content of the soft segment. As the molar ratio of TDI increases, the soft segment content decreases, resulting in a systematic rise in T_g from -49.6 °C to -17.7 °C. This upward shift in T_g indicates a corresponding reduction in the low-temperature resistance of the material.

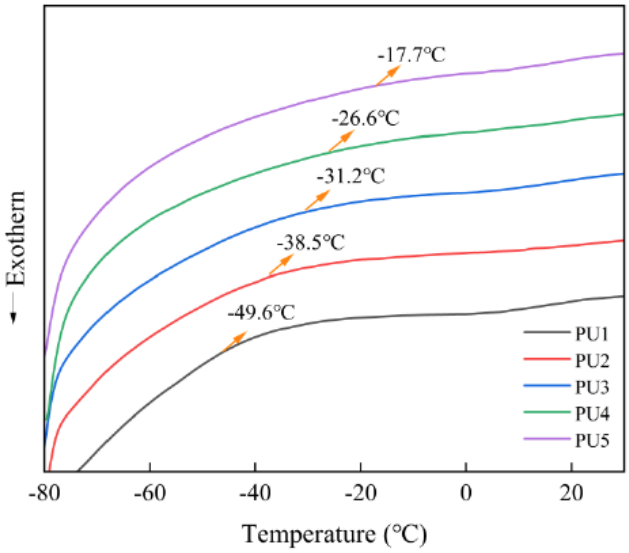

Figure 4: DSC curves of PU1 – PU5.

The mechanical properties of CPU elastomers with varying hard segment contents were evaluated through hardness, tensile and tear tests, with specific results summarized in Table **3** and Figure **5**. As the hard segment content (expressed as the molar ratio of n_{TDI}: $n_{PTMEG-1000}$) increases, the hardness of materials and tear strength exhibit a continuous rise, while the elongation at break gradually declines. In contrast, the tensile strength initially increases, reaching a maximum at n_{TDI}: $n_{PTMEG-1000}$ = 2: 1 (PU3), before subsequently decreasing. This behavior can be attributed to the increased presence of rigid segments within the polymer matrix, which enhances hardness but also introduces greater brittleness. The improved tear strength and reduced elongation at break are consistent with this structural change. The non-monotonic trend in tensile strength, with an optimum at the n_{TDI}: $n_{PTMEG-1000}$ = 2: 1 ratio, reflects a balance between enhanced stiffness and embrittlement induced by higher hard segment content.

Compared with CPUs made with traditional alcohol-based chain extenders (taking BDO as an example, the tensile strength of CPUs synthesized from TDI, PTMEG-1000 and BDO is 25-35 MPa, the tear strength is 70-90 N/mm, and the wear volume is 45-60 mm^3) [31], CPUs synthesized with MOCA as the chain extender have superior mechanical strength. This is mainly due to the rigid benzene ring structure in MOCA and the strong hydrogen bond effect of the urea group.

3.3. Influence of Hard Segment Composition on CPU Properties

As abovementioned, while the hard segment content plays a critical role in determining the properties of CPU elastomers, the chemical structure of the diisocyanate component also significantly influences material performance. Compared to TDI, MDI-based PUs generally exhibits superior mechanical properties and thermal stability, attributed to the more symmetric and rigid structure of the MDI hard segment. Furthermore, the lower vapor pressure of MDI reduces volatility during processing, contributing to safer and more controllable manufacturing. To systematically investigate these effects, a series of CPU elastomers were prepared with a constant hard-to-soft segment molar ratio (n_{NCO}: n_{OH} = 2: 1, corresponding to the

Table 3: Mechanical Properties of PU1 – PU5

	PU1	PU2	PU3	PU4	PU5
Hardness (Shore A)	80	84	87	89	91
Tensile strength (MPa)	39.64	42.36	50.74	47.20	44.10
Elongation at break (%)	420.23	395.95	388.24	381.15	344.23
300% tensile strength (MPa)	14.24	20.76	30.27	29.36	34.22
Tear strength (N/mm)	93.67	106.08	123.92	137.37	142.05

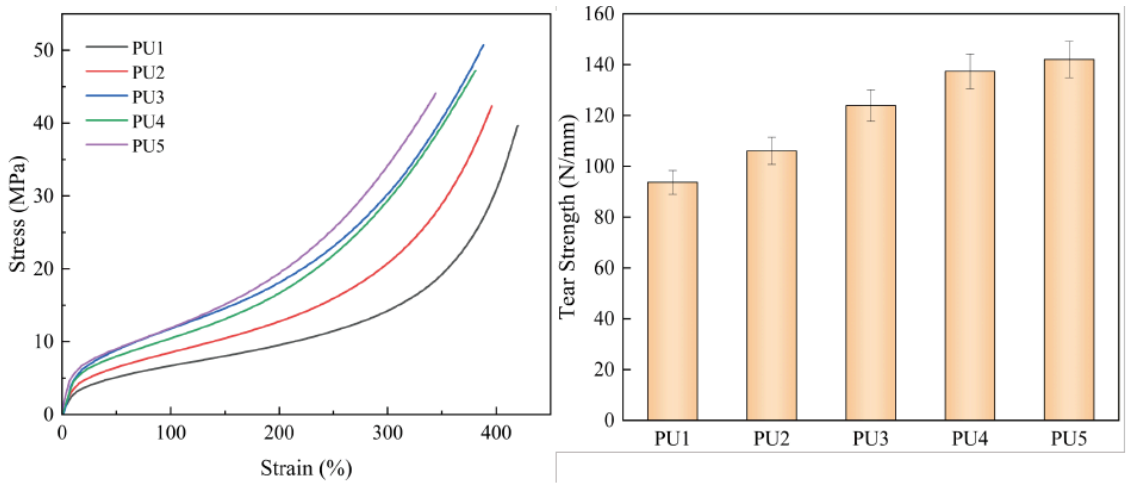

Figure 5: Stress-strain curves (**left**) and tear strength values (**right**) of PU1 – PU5.

optimal ratio identified in Section 3.2) while varying the TDI to MDI-50 molar ratio at 100:0, 70:30, 50:50, 30:70, and 0:100.

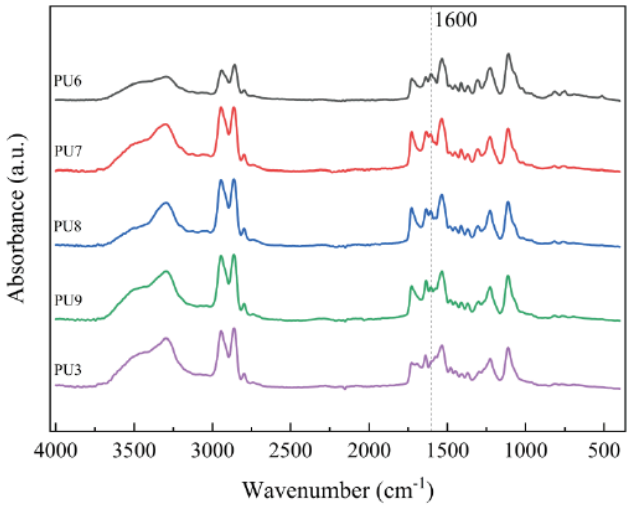

Figure 6: FTIR spectra of CPUs with different hard segment compositions.

Fourier transform infrared spectroscopy (FTIR) was used to characterize the chemical structures of CPU elastomers with different hard segment compositions (Figure **6**). The absence of any absorption around 2269 cm^{-1} confirms complete reaction of the -NCO groups. Aromatic ring skeletal vibrations are observed around 1600 cm^{-1}. With the increase of MDI-50 content, this band gradually splits into distinct features. The relatively sharp, single peak in the TDI-based sample (PU3) reflects the symmetric aromatic structure of TDI, whereas the split peaks observed in MDI-containing systems arise from the more asymmetric diphenylmethane unit, illustrating the distinct aromatic vibrational characteristics between the MDI and TDI hard segments.

The TGA and DTG curves of CPUs with different hard segment compositions are shown in Figure **7**. The pure MDI-50-based material (PU6) exhibits the highest initial decomposition temperature of 270°C, while the TDI-based sample (PU3) shows the lowest (240 °C). For the mixed MDI-50/TDI systems, the initial decomposition temperature progressively increases with higher MDI-50 content (PU7>PU8>PU9). Similarly, the temperature at the maximum decomposition rate is highest for the pure MDI-50-based sample (450 °C) and lowest for the pure TDI-based PU (435 °C). In blended systems, this maximum decomposition temperature gradually shifts toward that of the TDI-based material as the TDI proportion rises. The mass loss rates in the second and third decomposition stages (240-450 °C) do not differ significantly across the series. These results indicate that MDI-50-based CPUs possess slightly superior thermal stability relative

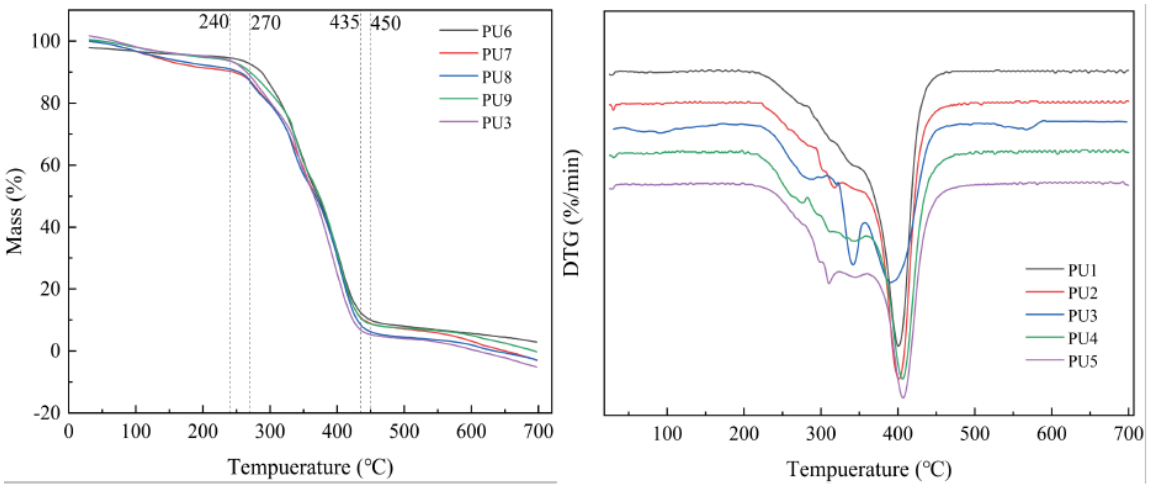

Figure 7: TGA curves (**left**) and DTG curves (**right**) of CPUs with different hard segment compositions.

to their TDI-based counterparts, although the overall influence on the thermal decomposition profile remains modest.

Figure **8** presents the DSC curves of CPU elastomers with different hard segment compositions, from which the corresponding glass transition temperatures (T_g) were determined. Contrary to the commonly observed trend, the T_g values exhibit a discernible decrease with increasing MDI-50 content, shifting from -31.2 °C for the pure TDI-based system to -36.7 °C for the pure MDI-50-based counterpart. This depression in T_g can be primarily attributed to the rigid benzene ring and regular symmetrical structure of MDI, it is easy to form regular spherical microcrystalline phase regions. Moreover, the formation of hydrogen bonds between long-chain molecules increases the degree of phase separation due to the tight aggregation of the corresponding segments. The improved phase purity allows the soft segment chains to move more freely, thereby lowering the glass transition temperature. Furthermore, the extended and linear architecture of the MDI-derived hard segments may reduce the degree of covalent cross-linking within the amorphous soft phase, contributing to the observed increase in chain mobility and consequent T_g reduction. Furthermore, although the NCO: OH molar ratio was fixed at 2: 1, the higher molecular weight of MDI-50 results in a slight increase in the hard segment content by mass fraction. Notably, the incorporation of MDI-50 ultimately leads to a lower glass transition temperature, suggesting that the resulting material can potentially maintain mechanical strength while being suitable for applications at lower temperatures.

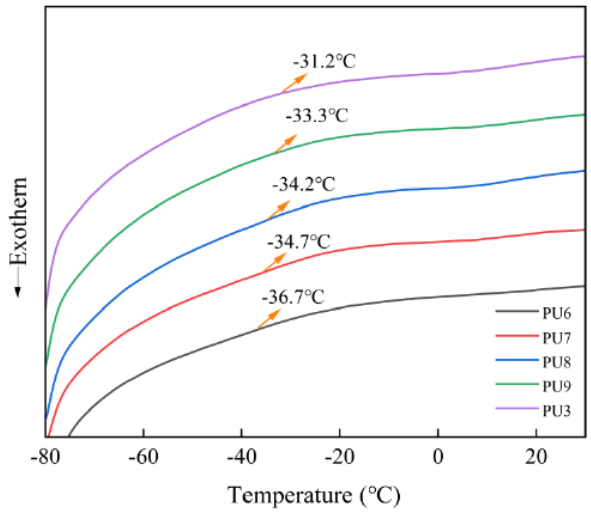

Figure 8: DSC curves of CPUs with different hard segment compositions.

The influence of different hard segment compositions on the mechanical properties of CPU including hardness, tensile and tear properties were evaluated and the corresponding results are summarized in Table **4** and Figure **9**. As the MDI-50 content increases, hardness and resilience show no clear monotonic trend, fluctuating between 85~87 Shore A and 44.6%~49.6%, respectively. Tensile strength and elongation at break reach optimal values in the MDI-50 and n_{MDI}: n_{TDI} = 3: 7 systems, with values of 46.35 MPa and 430%, respectively. Tear strength initially decreases and then increases with higher MDI-50 content, and the comprehensive mechanical performance is weakest at a molar ratio of n_{MDI}: n_{TDI} = 5: 5. The abrasion resistance is shown in Figure **10**. The results indicate that the lowest abrasion loss (17.75 mm^3) occurs at an n_{MDI}: n_{TDI} ratio of 7: 3 (PU7). In contrast, the pure MDI-50-based CPU exhibits an abrasion loss of 33.33 mm^3, approximately twice that of PU7. These findings demonstrate that the incorporation of a controlled amount of TDI into MDI-50-based CPUs can significantly enhance their abrasion performance. In general, the pure MDI-50-based CPU (PU6) exhibits a balanced combination of mechanical properties. At a blending molar ratio of n_{MDI}: n_{TDI} = 3: 7, tensile performance approaches that of the pure

Table 4: Mechanical Properties of CPUs with Different Hard Segment Compositions

	PU6	PU7	PU8	PU9	PU3
Hardness (Shore A)	87	87	85	86	87
Tensile strength (MPa)	46.35	42.84	35.96	45.74	42.47
Elongation at break (%)	429.88	380.6	321.03	430.98	329.95
300% tensile strength (MPa)	16.42	22.59	26.12	16.92	29.43
Tear strength (N/mm)	110.61	100.17	90.58	95.80	115.10
rebound resilience(%)	49.3	45.3	49.6	44.6	48
Detrition(mm^3)	33.33	17.75	21.48	26.76	24.09

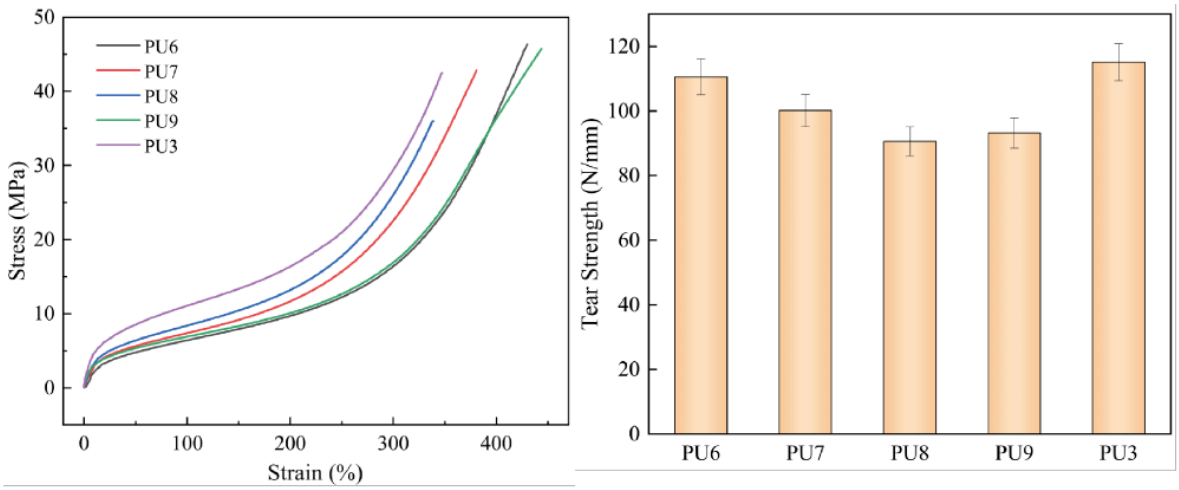

Figure 9: Stress-strain curves (**left**) and tear strength curves (**right**) of CPUs with different hard segment compositions.

MDI-50-based CPU, whereas tear resistance is markedly reduced. It is also noteworthy that TDI is susceptible to reaction with ambient moisture at room temperature, leading to potential performance deterioration, and exhibits higher volatility and toxicity compared with MDI-50. Therefore, CPUs prepared using MDI-50 and MOCA not only exhibit well-balanced mechanical properties but also offer improved processability and handling safety.

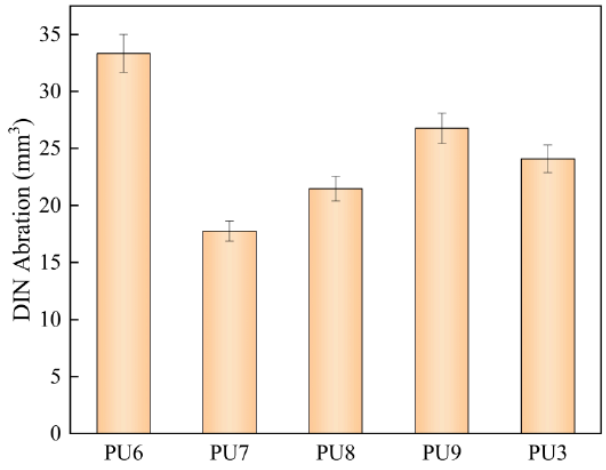

Figure 10: Abrasion performance of CPUs with different hard segment compositions.

The prepolymer based on PU6 formulation was chain-extended via the solvent method and subsequently cured at temperatures ranging from 110°C~140°C for 12 h. As shown in Figure **11**, the color of the resulting CPU samples progressively darkens from light to dark yellow with increasing curing temperature. Tensile data summarized in Table **5** reveal no significant variation in tensile strength across the temperature range, while the elongation at break shows a slight increasing trend at higher curing temperatures.

4. CONCLUSIONS

The key findings of this study demonstrate that the solvent-based approach effectively modulates the rapid reaction kinetics of molten MOCA, extending the pot life from less than 20 seconds to over 10 minutes while ensuring uniform processing. Optimization of the hard segment content reveals that a n_{TDI}: n_{PTMEG} ratio of 2: 1 delivers optimal tensile strength. Furthermore, the chemical structure of diisocyanates exerts a significant influence on performance: MDI-50-based CPUs exhibit superior thermal stability and a lower glass transition temperature due to enhanced microphase separation,

Table 5: Influence of Different Curing Temperatures on the Mechanical Properties of CPU

Curing temperature（℃）	110	120	130	140
Hardness (Shore A)	84	84	85	85
Tensile strength (MPa)	45.32	47.86	46.93	46.21
Elongation at break (%)	381.81	390.96	397.45	426.05

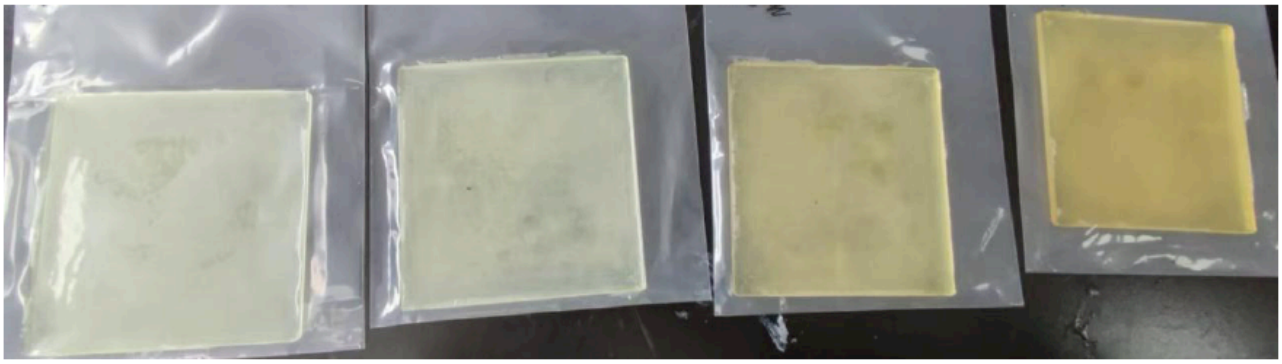

Figure 11: CPU Samples at Different Curing Temperatures (From left to right: 110°C, 120°C, 130°C, 140°C).

while TDI/MDI hybrid systems-particularly with a 7: 3 MDI: TDI ratio—achieve the best wear resistance. The novel contribution lies in clarifying the core regulatory mechanisms by which hard segment content and chemical composition govern the thermal, mechanical, and processing properties of MOCA-extended CPUs, establishing a multi-parameter synergistic optimization principle. Ultimately, this work provides a practical framework for customizing high-performance polyurethane elastomers, enabling the targeted design of specialized materials tailored to advanced application scenarios.

CONFLICTS OF INTEREST

The authors declare that they have no known competing financial interests or personal relationships that could have appeared to influence the work reported in this paper.

ACKNOWLEDGEMENTS

This work was supported by the National Natural Science Foundation of China (52572107), Natural Science Foundation of Chongqing, China (CSTB2025NSCQ-LZX0161), Shandong Provincial Natural Science Foundation Magnitude Fundamental Research, China (No. ZR2022ZD11), Natural Science Foundation of Shandong Province (ZR2023ME003).

REFERENCES

[1] Huynh TP, Haick H. Self-healing, fully functional, and multiparametric flexible sensing platform. Adv. Mater., 2016, 28(1): 138-143. https://doi.org/10.1002/adma.201504104

[2] Kuntz I. Anionic Polymerization. Kinetics, Mechanisms and synthesis, Organometallics, 1982, 1(8): 1106-1106. https://doi.org/10.1021/om00068a902

[3] Huang Q, Guo Z, Wu Z, Yuan C. Insight into the tribological performance of polyurethane composites under high temperature water lubrication, Tribol. Int., 2021, 155: 106784. https://doi.org/10.1016/j.triboint.2020.106784

[4] Chatrchyan S, Khachatryan V, Sirunyan AM, Tumasyan A, Ceard L. Study of high-p(T) charged particle suppression in PbPb compared to pp collisions at root s(NN)=2.76 TeV. Eur. Phys. J. C, 2012, 72(3): 1945. https://doi.org/10.48550/arXiv.1202.2554

[5] Vassallo E, Cremona A, Laguardia L, Mesto E. Preparation of plasma-polymerized SiOx-like thin films from a mixture of hexamethyldisiloxane and oxygen to improve the corrosion behaviour. Surf. Coat. Technol., 2006, 200: 3035-3040. https://doi.org/10.1016/j.surfcoat.2004.11.001

[6] Akindoyo JO, Beg MH, Ghazali S, Islam MR, Jeyaratnam N, Yuvaraj AR. Polyurethane types, synthesis and applications - a review. RSC Adv., 2016, 6(115): 114453-114482. https://doi.org/10.1039/C6RA14525F

[7] Prisacariu C., Polyurethane elastomers: from morphology to mechanical aspects. Springer Science & Business Media, 2011. https://doi.org/10.1007/978-3-7091-0514-6

[8] Pukánszky Jr B, Bagdi K, Tóvölgyi Z, Varga J, Botz L, Hudak S, Dóczi T, Pukánszky B. Nanophase separation in segmented polyurethane elastomers: Effect of specific interactions on structure and properties. Eur. Polym. J., 2008, 44(8): 2431-2438. https://doi.org/10.1016/j.eurpolymj.2008.06.008

[9] Zia KM, Barikani M, Zuber M, Bhatti IA, Sheikh MA. Molecular engineering of chitin based polyurethane elastomers. Carbohydr. Polym., 2008, 74(2): 149-158. https://doi.org/10.1016/j.carbpol.2008.03.013

[10] Xiaojuan L, Xiaorui L, Lei W, Yiding S. Synthesis and characterizations of waterborne polyurethane modified with 3-aminopropyltriethoxysilane. Polym. Bull., 2010, 65(1): 45-57. https://doi.org/10.1007/s00289-009-0233-x

[11] Senichev VY, Pogoreltsev EV. Relationship between the Abrasion Resistance of Urethane-Containing Elastomers and Their Structure. Polym. Sci. Ser. D, 2023, 16(3): 549-552. https://doi.org/10.1134/S1995421223030309

[12] Chern YC, Hsieh KH, Hsu JS. Interpenetrating polymer networks of polyurethane cross-linked epoxy and polyurethanes. J. Mater. Sci., 1997, 32(13): 3503-3509. https://doi.org/10.1023/A:1018645405853

[13] Park JB, Jeong JH, Lee M, Lee DY, Byun Y. Xenotransplantation of exendin-4 gene transduced pancreatic islets using multi-component (alginate, poly-L-lysine, and polyethylene glycol) microcapsules for the treatment of type 1 diabetes mellitus. J. Biomater. Sci. Polym. Ed., 2013, 24(18): 2045-2057. https://doi.org/10.1080/09205063.2013.823071

[14] Xu Q, Guo Z, Huang Q, Yuan C. Effects of soft chain materials on the tribological performances of thermosetting polyurethane under water-lubrication. Tribol. Int., 2024, 196: 12. https://doi.org/10.1016/j.triboint.2024.109692

[15] Liang X, Guo Z, Tian J, Yuan C. Development of modified polyacrylonitrile fibers for improving tribological performance characteristics of thermoplastic polyurethane material in water-lubricated sliding bearings. Polym. Adv. Technol., 2020, 31(12): 3258-3271. https://doi.org/10.1002/pat.5050

[16] Sukumar P, Jayashree V, Nair MRG, Nair MNR. Synthesis and thermal studies of block copolymers from NR and MDI-based polyurethanes. J. Appl. Polym. Sci., 2009, 111(1): 19-28. https://doi.org/10.1002/app.27300

[17] Luo H, Deng H, Zhu Y, Shi H, Zhang C, Wang Y. High-performance polyurethane elastomers with mechano-responsive self-reinforcing via rigid-flexible segments regulation. Compos. B: Eng., 2025, 297: 112-287. https://doi.org/10.1016/j.compositesb.2025.112287

[18] International Agency for Research on Cancer. Schistosomes, liver flukes and Helicobacter pylori. IARC Working Group on the Evaluation of Carcinogenic Risks to Humans. Lyon, 7–14. IARC Monogr. Eval. Carcinog. Risks Hum. 1994, 61: 1.

[19] Malucelli G, Priola A, Ferrero F, Quaglia A, Frigione M, Carfagna C. Polyurethane resin-based adhesives: curing reaction and properties of cured systems. Int. J. Adhes. Adhes., 2005, 25(1): 87-91. https://doi.org/10.1016/j.ijadhadh.2004.04.003

[20] Kuo L, Luijten BJ, Li S, De Moraes AC, Silvaroli AJ, Wallace SG, Hui J, Downing JR, Shull KR, Hersam MC. Sterilizable and reusable UV-resistant graphene–polyurethane elastomer composites. ACS Appl. Mater. Interfaces, 2022, 14(47): 53241-53249. https://doi.org/10.1021/acsami.2c17791

[21] Rymuza Z, Misiak M, Kuhn L, Schmidt-Szałowski K, Rżanek-Boroch Z. Control tribological and mechanical properties of MEMS surfaces. Part 2: nanomechanical behavior of self-lubricating ultrathin films. Microsyst. Technol., 1999, 5(4): 181-188. https://doi.org/10.1007/s005420050161

[22] Zhang M, King R, Hanes M, James SP. A novel ultra high molecular weight polyethylene–hyaluronan microcomposite for use in total joint replacements. I. Synthesis and physical/chemical characterization. J. Biomed. Mater. Res. Part A, 2006, 78(1): 86-96. https://doi.org/10.1016/j.compositesa.2008.10.003

[23] Liu X, Du P, Liu L, Zheng Z, Wang X, Joncheray T, Zhang Y. Kinetic study of Diels–Alder reaction involving in maleimide–furan compounds and linear polyurethane. Polym. Bull., 2013, 70(8): 2319-2335. https://doi.org/10.1007/s00289-013-0954-8

[24] Xiong J, Liu Y, Yang X, Wang X. Thermal and mechanical properties of polyurethane/montmorillonite nanocomposites based on a novel reactive modifier. Polym. Degrad. Stab. 2004, 86(3): 549-555. https://doi.org/10.1016/j.polymdegradstab.2004.07.001

[25] Yang JH, Chun BC, Chung YC, Cho JH. Comparison of thermal/mechanical properties and shape memory effect of polyurethane block-copolymers with planar or bent shape of hard segment. Polymer, 2003, 44(11): 3251-3258. https://doi.org/10.1016/S0032-3861(03)00260-X

[26] Geng L, Qiao Y, Sun R, Guo L, Li ZQ, Ma Y, Yu MH, Chang Z, Bu XH. Solution-Processable Metal-Organic Framework Featuring Highly Tunable Dynamic Aggregation States. Adv. Mater, 2025, 37(4): 2415511. https://doi.org/10.1002/adma.202415511

[27] Huyan C., Liu D., Pan C., Wang D., Guo Z., Zhang X, Dai S, Xu BB, Chen F. Thermally recyclable and reprocessable glass fiber reinforced high performance thermosetting polyurethane vitrimer composites. Chem. Eng. J, 2023, 471: 144478. https://doi.org/10.1016/j.cej.2023.144478

[28] Zhou N, Wang HY, Liu SQ, Cao G, Liu YN. Additive-free morphology controlled synthesis of hierarchical lithium iron phosphate mesosturctures. Int. J. Electrochem. Sci., 2013, 8(7): 9149-9162. https://doi.org/10.1016/S1452-3981(23)12956-7

[29] Stern T. Conclusive chemical deciphering of the consistently occurring double-peak carbonyl-stretching FTIR absorbance in polyurethanes. Polym. Adv. Technol., 2019, 30(3): 675-687. https://doi.org/10.1002/pat.4503

[30] Geng Z, Pang A, Ding T, Guo X, Yang R, Luo Y, Zhai J. Overlooked impact of interchain H-bonding between cross-links on the mechanical properties of thermoset polyurethane elastomers. Macromolecules, 2022, 55(19): 8749-8756. https://doi.org/10.1021/acs.macromol.2c00873

[31] Hinrichsen, G. Urethane Elastomers/Liquid Crystalline Polyurethane Blends. Adv. Urethane Sci. Technol., 1996, 13: 140. https://doi.org/10.1002/adv.1994.060130105